

High cell diversity and complex peptidergic signalling underlie placozoan behaviour

Frédérique Varoquaux¹, Elizabeth A. Williams², Susie Grandemange¹, Luca Truscillo¹, Kai Kamm³, Bernd Schierwater³, Gáspár Jékely^{2,4,5}, Dirk Fasshauer^{1,4}

¹Department of Fundamental Neurosciences, University of Lausanne, Rue du Bugnon 9, CH-1005 Lausanne, Switzerland

² Living Systems Institute, University of Exeter, Stocker road, EX44QD Exeter, United Kingdom

³ITZ, Ecology and Evolution TiHo Hannover, Bünteweg 17d, 30559 Hannover, Germany

⁴Corresponding authors

⁵Lead contact

Correspondence: G.Jekely@exeter.ac.uk (GJ), dirk.fasshauer@unil.ch (DF)

SUMMARY

Placozoans, together with sponges, are the only animals devoid of a nervous system and muscles, yet both respond to sensory stimulation in a coordinated manner. How behavioural control in these free-living animals is achieved in the absence of neurons and, more fundamentally, how the first neurons evolved from more primitive cells for communication during the rise of animals is not yet understood [1-5]. The placozoan *Trichoplax adhaerens* is a millimeter-wide, flat, free-living marine animal composed of six morphologically identified cell types distributed across a simple bodyplan [6-9]: a thin upper epithelium and a columnar lower epithelium interspersed with a loose layer of fiber cells in between. Its genome contains genes encoding several neuropeptide-precursor-like proteins and orthologs of proteins involved in neurosecretion in animals with a nervous system [10-12]. Here we investigate peptidergic signalling in *Trichoplax adhaerens*. We found specific expression of several neuropeptide-like molecules in non-overlapping cell populations distributed over the three cell layers, revealing an unsuspected cell-type diversity of *Trichoplax adhaerens*. Using live imaging, we discovered that treatments with 11 different peptides elicited striking and consistent effects on the animals' shape, patterns of movement and velocity that we categorized under three main types: (i) crinkling, (ii) turning, and (iii) flattening and churning. Together, the data demonstrate a crucial role for peptidergic signalling in nerveless placozoans and suggest that peptidergic volume signalling may have predated synaptic signalling in the evolution of nervous systems.

KEYWORDS

Animal evolution, cnidarians, ctenophores, early metazoans, nervous system evolution, placozoans, peptidergic signalling, porifera, *Trichoplax adhaerens*

RESULTS AND DISCUSSION

***Trichoplax adhaerens* comprises multiple populations of peptide-secreting cells**

Peptidergic communication is widely used throughout most of the animal kingdom. It may even predominate neural communication in phyla such as cnidarians and ctenophores [11,13]. The importance of secreted peptides in placozoan physiology and behaviours is not known. The genome of *T. adhaerens* encodes for determinants of both classical and peptidergic (neuro-)transmission [10-12]. Among the putative peptide signalling-molecules predicted from the genome [11,12], we selected candidates with good antigenic profiles to generate antibodies. We chose five peptides bearing an amidation site (SIFGamide, SITFamide, YYamide, RWamide and FFNPamide) as well as one of the four predicted insulin-like peptides, TrIns3. Immunostainings with the affinity purified antibodies in whole-mount *T. adhaerens* uncovered six populations of cells with distinct distribution patterns (Figure 1A-C). Upon co-labelling experiments [14], these peptides were never found to be co-expressed, as illustrated for SIFGamide, SITFamide and FFNPamide (Figure 1B) and SITFamide, FFNPamide and TrIns3 (Figure S1). Instead, it appears that each of the six populations of peptide-secreting cells spreads concentrically, delineating distinct territories (Figure 1C). Starting from the outside of the animal towards its inside, SIFGamide immunoreactive cells are found at the very edge and the outer rim of the upper epithelium. SITFamide cells distribute further inwards in the upper epithelium, in an equally broad annular area. Together, the description of these populations validates and refines the suggested rim-vs-centre cell composition of *T. adhaerens* [7,8]. Intriguingly, TrIns3-labelled cells are located in the lower epithelium along a thin ring across the boundaries of the SIFGamide and SITFamide territories. A few, small TrIns3-reactive cells are at times also found at the edge.

Earlier studies using antibodies against RFamide [15] or FMRFamide [8] have identified putative peptidergic cells at the rim. Ciliated, endocrine-like cells with neurosecretory features (e.g. expressing SNARE proteins) have also previously been described at the rim and named gland cells [6-8]. Since no FMRFamide peptide precursor could be identified in the *T. adhaerens* genome, we asked whether labelling with anti-FMRFamide antibodies could derive from cross-reactivity with (some of) the populations of newly-identified cells. Upon co-immunolabelling with commercial anti-FMRFamide antibodies, we observed indeed that SITFamide-expressing cells and, more faintly, TrIns3-expressing cells are also labelled by these antibodies. Anti-FMRF antibodies also label cells near the rim of the animal that are not labelled by any of the tested antibodies. These observations suggest that anti-FMRFamide antibodies detect SITFamide and maybe other peptides (Figure S1).

The remaining three populations of peptide-secreting cells, expressing RWamide, FFNPamide and YYamide distributed away from the rim in more central parts of the organism. Labelling for RWamide is confined to the inside of the organism and does not reach to the surface. The fluorescent peptidergic granules distribute tightly around a rather small nucleus located deep in the middle of the organism. Since they are not observed in correlation with autofluorescent particles nor with large nuclei or cell-bodies, we suggest that RWamide-secreting cells do not correspond to the large and complex fiber cells, landmark of the intermediate, non-epithelial layer [7,8] but to another, as yet unidentified cell type. RWamide cells spread within a very large ring, sometimes even to the centre of the organism (Figure 1C). Finally, cells expressing FFNPamide and YYamide mix and mingle in the centre part of the lower epithelium. FFNPamide cells are thin and tall and more abundant than YYamide cells, while the

latter appear larger and filled with numerous labelled granules. In this region, cylindrical epithelial cells, lipophil cells and another population of putative endocrine cells (labelled with SNAREs but not FMRFamide antibodies) have been reported [7,8]. Whether FFNPamide and/or YYamide-cells may correspond to SNARE-expressing cells cannot be addressed currently since available antibodies did not allow for double-labelling. *T. adhaerens*' genome encodes several isoforms of secretory SNARE proteins [16], and the specificity of antibodies used so far is unclear. It is likely that different populations of secretory cells with different sets of secretory SNARE protein isoforms exist in *T. adhaerens*.

In summary, we uncovered an unexpected diversity of peptidergic cells with unique concentric distribution patterns (Figure 1C) in this morphologically simple animal. This suggests that secreted peptides have unique signalling functions potentially regulating many aspects of *T. adhaerens* physiology.

Neuropeptide-like molecules elicit strong stereotypical behaviours in *Trichoplax adhaerens*

Placozoans move slowly across surfaces using a densely ciliated lower epithelium [9]. They produce stereotypical behaviours as they flip, fold, flatten, rotate and constantly change their shape [17-20] in a highly coordinated manner. The animals also change their speed as a function of light intensity [19] or presence of food [8,18,19,21-23]. Their extra-organismal feeding behaviour is particularly complex [18,21]. How *T. adhaerens* coordinates such movements is only beginning to emerge.

To test the effects of peptides on *T. adhaerens*' behaviour, we recorded over 50 min the motor behaviour of several individuals. At 15 min, we applied each one of eleven synthetic peptides predicted from *T. adhaerens* neuropeptide-precursor-like proteins. We tested the peptides ELPE, FFNPamide, LF, LFNE, MFPP, PWN, RWamide, SIFGamide, SITFamide, WPPF and YYamide (Tables S1 & S2; note that ELPE and MFPP have not been reported so far). We used peptides at varying concentrations across trials (200 nM to 50 μ M; Table S1; in-depth analysis was performed for 20 μ M peptide). We observed strong effects on behaviour following peptide treatment, indicating that the peptides reached their targets, as expected from the anatomy of the organism [22]. Several parameters including the area and shape (roundness) of the organisms, as well as locomotion speed and path trajectories were scored. The timing and extent of individual responses varied considerably, making it impractical to reflect the effects in averaged datasets. Hence we show averaged and individual responses as appropriate depending on the nature of the effect of each peptide.

In the majority of cases, the peptides elicited strong and characteristic changes in movement. We categorized these changes under three general types: (i) crinkling, (ii) rounding up and rotating, and (iii) flattening and churning.

Upon application of PWN, *T. adhaerens* immediately crinkled, as reflected by a sharp decrease in the area of the animals. The effect lasted for approximately 10 minutes, after which the animals recovered their normal shape (Figure 2A, C-D; Movie S1). Application of SIFGamide induced even stronger crinkling that led to an approximate 50 % decrease in the area, an effect from which the animals only started to recover by the end of the recording (Figure 2E, G-H). In addition, SIFGamide-treated animals often detached from the substrate (Movie S2). Detachment was briefly reported elsewhere [24]. *T. adhaerens* adopts a similar shape in response to UV light [25] or when flushed with a strong water stream.

The application of LF and LFNE peptides triggered a different type of morphological and behavioural change. Both peptides induced the animals to rotate for several minutes around a fixed axis (arrows in Figure 3E) or to move in circular trajectories (Figure 3B, F; Movies S3 & S4). They transiently flattened, while keeping their round shape, to reach up to 240 % (LF; Figure 3D) or 130 % (LFNE; Figure 3H) of their average area. Upon LF application, animals rapidly adopted a smooth round shape (Figure 3A) and rotated around themselves and in the dish. While the animals recovered, their edges were seen undulating at times. Upon LFNE application, the majority of animals rounded up, often adopting a spiral shape (Figure 3E) and turned around themselves (Figure 3F). A few individuals elongated or undulated at the edges.

Another group of peptides, comprising FFNPamide, ELPE, MFPPF and WPPF, induced actions reminiscent of feeding behaviour, without entirely recapitulating the feeding sequence (Movies S5-8). When feeding, *T. adhaerens* stops moving before a large fringe of its periphery stretches and flattens down, adhering to the bottom. Meanwhile, its central part undergoes coordinated rhythmic movements including stretching, contracting and rotating components ("churning" [18,21]). The animal then loosens itself from the bottom and resumes crawling. All four peptides increased the number of flattening events (Figure 4C, G, K, O), as shown by an increase in average area (Figure S2). Most often, flattening and pausing events occurred concomitantly (Figure 4B vs. D, J vs. L, N vs. P), while they were occasionally slightly shifted (Figure 4F vs. H). Flattening induced by FFNP was extreme, as the centre part of the organism appeared extremely pale. This suggests that the animal is able to thin out to an extent that has not been reported before - up to 5 times its "default" size. ELPE, MFPPF and WPPF induced the animals to adhere more tightly to the dish at their rim (which hence appears paler (Figure 4E, I, M)), to flatten down and to churn with slightly different movements. In the presence of MFPPF, animals churn slower or faster than untreated animals, and for extended periods of time. FFNPamide addition also triggered moderate churning movements. Interestingly, the numerous FFNPamide-immunoreactive cells embedded in the lower epithelium (Figure 1) are found in the same area as the digestive enzyme-releasing lipophil cells [8,21], hence are well positioned to fulfil a role in modulating feeding behaviour [4,26]. Altogether, these behaviours could be subprograms of the motor alterations associated with the food uptake process. Whether the peptides involved are acting independently, sequentially or in synergy requires further investigation.

Finally, a few peptides induced only subtle alterations in *T. adhaerens* behaviour (Figure S3; Movies S9-11). Neither SITFamide, YY, nor different RWamide peptides affected the flattening rate of the animals. SITFamide induced an effect which was difficult to quantify. The speed of the animals was significantly lower during the 30 minutes monitored after SITFamide application. Some animals slowed down (Figure S3D) without stopping (Figure S3A, B). In one case, an animal stopped but did not flatten (2_102, Figure S3). Application of YYamide resulted in a small but significant increase in the speed of or the distance travelled by the animals during the later phase of the recordings (Figure S2G). In one case, an animal increased its area without slowing down (1_128, Figure S3). Finally, the effects of RWamides were tested in a pilot series of experiments using the three slightly different peptides RWamide1, RWamide2, RWamide3 and their respective forms bearing a N-terminal pyroGlutamine modification pGluRWamide1, pGluRWamide2 and pGluRWamide3. No drastic effect was observed over the 30 minutes of recordings. Hence, pRWamide2 was arbitrarily selected for further trials. No change

in area, trajectory, speed or distance travelled was noted. Application of the vehicle alone did not alter the animals' behaviour (Figure S4; Movies S12; S13).

Overall, our data show that most predicted peptides are able to strongly alter *T. adhaerens* behaviour. This suggests that peptidergic signalling pathways that can affect the animals' contractility and movements are in place. Moreover, we describe a previously undocumented capacity of extreme physical alterations of *T. adhaerens*, from extreme flattening to crinkling and from churning to rotating. Our results suggest that motor behaviours in *T. adhaerens* likely result from the coordinated interplay of several cellular arrays that are under the strong influence of peptidergic signals.

An earlier study reports that gland cells secrete an endomorphin-like peptide (TaELP), which arrests ciliary beating, inducing feeding-like pauses [24] (Figure S5). Interestingly, we observed that the application of the endomorphin-like peptide also induced flattening but no churning (Table S1). At lower concentrations, crinkling was observed, whereas high concentrations caused the animal to rotate. Changes in movement may rely in part on changes in ciliary beating. Flattening may be generated by fast contractions of epithelial cells [20] or by contractions of the large, actin/microtubule-rich fiber cells. These are located in between the two epithelial layers [26,27] and are connected to each other and contact all cell types [8].

Peptide signalling molecules and their respective receptors appeared early in metazoan evolution and have been described in all animals with a nervous system including ctenophores [13,28] and cnidarians. Our study suggests that peptide signalling molecules play an important role in cell-cell communication in *T. adhaerens* as well. Of note, the genome of *T. adhaerens* encodes a rich repertoire of G-protein coupled receptors [10,29], at least some of which likely act as receptors for the peptides characterised in this study [11]. The peptide signalling systems in *T. adhaerens* are less complex than those of eumetazoans and might thus represent a more ancestral stage [11]. It will be interesting to explore the occurrence and actions of peptide signalling molecules in other placozoans [30,31]. Since the *T. adhaerens* genome also contains all determinants of transmission via classical neurotransmitters [10], it will be essential to scrutinize whether the animal combines elements of peptide and classical transmission. The peptide-containing cells described herein might represent specialized, non-neuronal secretory cells or neuroendocrine-like/neuron-like cells. These cell may be able to co-release both types of transmitters as is found in neurons and endocrine cells in animals with nervous systems [32].

Altogether, our data demonstrate that cell-type diversity in placozoans is higher than previously inferred [7,8] and that several specialized cell types, regarded as the "basal building blocks of multicellular organisms" [33], have already emerged in this phylum. Indeed, a recent single-cell transcriptome study also revealed the presence of several hitherto unexplored lower-frequency cell types expressing unique signalling peptides [34] (Figure S6). In *T. adhaerens*, several populations of topographically organized peptide-secreting cells can strongly modulate the animals' movements. Our results suggest that peptidergic signalling is an important mode of communication for placozoans, as is the case for cnidarians and bilaterians [11,35-39].

ACKNOWLEDGMENTS

This work was supported by the Swiss National Science Foundation (Marie-Heim Vögtlin grant PMPDP3_158377 to FV and grant 31003A_160343 to DF). EAW was supported by a grant from the DFG - Deutsche Forschungsgemeinschaft (Reference no. JE 777/1). We thank Yves Mingard, Dominique Trauffer, and Marie-Laure Gadolini for taking care of our *Trichoplax* lines and technical assistance, and Mathieu Künzi for support with analysis and reading of the manuscript.

AUTHOR CONTRIBUTIONS

FV, EW, GJ, DF designed the study; FV, EW, LT, SG performed experiments; KK, BS provided strain and advice; FV, EW, LT, SG, BS, GJ, DF analysed data; FV, EW, GJ, DF wrote the paper and all authors reviewed, commented on, and edited the manuscript.

DECLARATION OF INTERESTS

The authors declare no competing financial interests.

REFERENCES

- [1] Jorgensen EM. Animal evolution: looking for the first nervous system. *Current Biology* 2014;24:R655–8. doi:10.1016/j.cub.2014.06.036.
- [2] Arendt D, Benito-Gutierrez E, Brunet T, Marlow H. Gastric pouches and the mucociliary sole: setting the stage for nervous system evolution. *Philos Trans R Soc Lond B Biol Sci* 2015;370. doi:10.1098/rstb.2015.0286.
- [3] Hartenstein V, Stollewerk A. The evolution of early neurogenesis. *Dev Cell* 2015;32:390–407. doi:10.1016/j.devcel.2015.02.004.
- [4] Varoqueaux F, Fasshauer D. Getting Nervous: An Evolutionary Overhaul for Communication. *Annu Rev Genet* 2017. doi:10.1146/annurev-genet-120116-024648.
- [5] Liebeskind BJ, Hofmann HA, Hillis DM, Zakon HH. Evolution of Animal Neural Systems. *Annu Rev Ecol Evol Syst* 2017;48:377–98. doi:10.1146/annurev-ecolsys-110316-023048.
- [6] Schulze FE. Über *Trichoplax adhaerens*. *Abh D Kgl Preuss Akad D Wiss Zu Berlin* 1892:1–23.
- [7] Grell K, Benwitz G. Die Ultrastruktur von *Trichoplax adhaerens* FE Schulze. *Cytobiologie* 1971;4:216–40.
- [8] Smith CL, Varoqueaux F, Kittelmann M, Azzam RN, Cooper B, Winters CA, Eitel M, Fasshauer D, Reese TS. Novel Cell Types, Neurosecretory Cells, and Body Plan of the Early-Diverging Metazoan *Trichoplax adhaerens*. *Current Biology* 2014;24:1565–72. doi:10.1016/j.cub.2014.05.046.
- [9] Schierwater B, DeSalle R. Placozoa. *Current Biology* 2018;28:R97–8. doi:10.1016/j.cub.2017.11.042.
- [10] Srivastava M, Begovic E, Chapman J, Putnam NH, Hellsten U, Kawashima T, Kuo A, Mitros T, Salamov A, Carpenter ML, et al. The *Trichoplax* genome and the nature of placozoans. *Nature* 2008;454:955–60. doi:10.1038/nature07191.

- [11] Jékely G. Global view of the evolution and diversity of metazoan neuropeptide signaling. *Proc Natl Acad Sci USA* 2013;110:8702–7. doi:10.1073/pnas.1221833110.
- [12] Nikitin M. Bioinformatic prediction of *Trichoplax adhaerens* regulatory peptides. *Gen Comp Endocrinol* 2015;212:145–55. doi:10.1016/j.ygcen.2014.03.049.
- [13] Jékely G, Paps J, Nielsen C. The phylogenetic position of ctenophores and the origin(s) of nervous systems. *Evodevo* 2015;6:1. doi:10.1186/2041-9139-6-1.
- [14] Conzelmann M, Jékely G. Antibodies against conserved amidated neuropeptide epitopes enrich the comparative neurobiology toolbox. *Evodevo* 2012;3. doi:10.1186/2041-9139-3-23.
- [15] Schuchert P. *Trichoplax adhaerens* (Phylum Placozoa) has Cells that React with Antibodies Against the Neuropeptide RFamide. *Acta Zoologica* 1993;74:115–7. doi:10.1111/j.1463-6395.1993.tb01227.x.
- [16] Kloepper TH, Kienle CN, Fasshauer D. SNAREing the basis of multicellularity: consequences of protein family expansion during evolution. *Mol Biol Evol* 2008;25:2055–68. doi:10.1093/molbev/msn151.
- [17] Kuhl W, Kuhl G. Untersuchungen über das Bewegungsverhalten von *Trichoplax adhaerens* F. E. Schulze (Zeittransformation: Zeitraffung). *Zoomorphology* 1966;56:417–35. doi:10.1007/BF00442291.
- [18] Ueda T, Koya S, Maruyama YK. Dynamic patterns in the locomotion and feeding behaviors by the placozoan *Trichoplax adhaerence*. *BioSystems* 1999;54:65–70.
- [19] Heyland A, Croll R, Goodall S, Kranyak J, Wyeth R. *Trichoplax adhaerens*, an enigmatic basal metazoan with potential. *Methods Mol Biol* 2014;1128:45–61. doi:10.1007/978-1-62703-974-1_4.
- [20] Armon S, Bull MS, Aranda-Diaz AJ, Prakash M. Ultra-fast cellular contractions in the epithelium of *T. adhaerens* and the “active cohesion” hypothesis. *bioRxiv* 2018:258103. doi:10.1101/258103.
- [21] Smith CL, Pivovarova N, Reese TS. Coordinated Feeding Behavior in *Trichoplax*, an Animal without Synapses. *PLoS ONE* 2015;10:e0136098. doi:10.1371/journal.pone.0136098.
- [22] Smith CL, Reese TS. Adherens Junctions Modulate Diffusion between Epithelial Cells in *Trichoplax adhaerens*. *Biol Bull* 2016;231:216–24. doi:10.1086/691069.
- [23] Smith CL, Abdallah S, Wong YY, Le P, Harracksingh AN, Artinian L, Tamvacakis AN, Rehder V, Reese TS, Senatore A. Evolutionary insights into T-type Ca²⁺ channel structure, function, and ion selectivity from the *Trichoplax adhaerens* homologue. *J Gen Physiol* 2017;204:jgp.201611683. doi:10.1085/jgp.201611683.
- [24] Senatore A, Reese TS, Smith CL. Neuropeptidergic integration of behavior in *Trichoplax adhaerens*, an animal without synapses. *J Exp Biol* 2017;220:3381–90. doi:10.1242/jeb.162396.
- [25] Pearse VB. Growth and behavior of *Trichoplax adhaerens*: first record of the phylum Placozoa in Hawaii. *Pacific Science* 1989;43:117–21. doi:1534-6188.
- [26] Grell KG, Benwitz G. [Special connecting structures between fiber cells of *Trichoplax adhaerens* F. E. Schulze (author's transl)]. *Z Naturforsch, C, Biosci* 1974;29:790.

- [27] Behrendt G, Ruthmann A. The cytoskeleton of the fiber cells of *Trichoplax adhaerens* (Placozoa). *Zoomorphology* 1986;106:123–30. doi:10.1007/BF00312114.
- [28] Moroz LL, Kocot KM, Citarella MR, Dosung S, Norekian TP, Povolotskaya IS, Grigorenko AP, Dailey C, Berezikov E, Buckley KM, et al. The ctenophore genome and the evolutionary origins of neural systems. *Nature* 2014;510:109–14. doi:10.1038/nature13400.
- [29] Krishnan A, Mustafa A, Almén MS, Fredriksson R, Williams MJ, Schiöth HB. Evolutionary hierarchy of vertebrate-like heterotrimeric G protein families. *Mol Phylogenet Evol* 2015;91:27–40. doi:10.1016/j.ympev.2015.05.009.
- [30] Eitel M, Osigus H-J, DeSalle R, Schierwater B. Global diversity of the placozoa. *PLoS ONE* 2013;8:e57131. doi:10.1371/journal.pone.0057131.
- [31] Eitel M, Francis W, Osigus H-J, Krebs S, Vargas S, Blum H, Williams GA, Schierwater B, Wörheide G, et al. A taxogenomics approach uncovers a new genus in the phylum Placozoa. *bioRxiv* 2017:202119. doi:10.1101/202119.
- [32] Nusbaum MP, Blitz DM, Marder E. Functional consequences of neuropeptide and small-molecule co-transmission. *Nat Rev Neurosci* 2017;18:389–403. doi:10.1038/nrn.2017.56.
- [33] Arendt D, Musser JM, Baker CVH, Bergman A, Cepko C, Erwin DH, Pavlicev M, Schlosser G, Widder S, Laubichler MD, et al. The origin and evolution of cell types. *Nat Rev Genet* 2016;17:744–57. doi:10.1038/nrg.2016.127.
- [34] Sebé-Pedrós A, Chomsky E, Pang K, Lara-Astiaso D, Gaiti F, Mukamel Z, Amit I, Hejnal A, Degnan BM, Tanay A. Early metazoan cell type diversity and the evolution of multicellular gene regulation. *Nat Ecol Evol* 2018;2:1176–88. doi:10.1038/s41559-018-0575-6.
- [35] Mirabeau O, Joly J-S. Molecular evolution of peptidergic signaling systems in bilaterians. *Proc Natl Acad Sci USA* 2013;110:E2028–37. doi:10.1073/pnas.1219956110.
- [36] Grimmelhuijzen CJP, Hauser F. Mini-review: the evolution of neuropeptide signaling. *Regul Pept* 2012;177 Suppl:S6–9. doi:10.1016/j.regpep.2012.05.001.
- [37] Bosch TCG, Klimovich A, Domazet-Lošo T, Gründer S, Holstein TW, Jékely G, Miller DJ, Murillo-Rincon AP, Rentzsch F, Richards GS, et al. Back to the Basics: Cnidarians Start to Fire. *Trends Neurosci* 2017;40:92–105. doi:10.1016/j.tins.2016.11.005.
- [38] Williams EA, Verasztó C, Jasek S, Conzelmann M, Shahidi R, Bauknecht P, Mirabeau O, Jékely G. Synaptic and peptidergic connectome of a neurosecretory centre in the annelid brain. *Elife* 2017;6. doi:10.7554/eLife.26349.
- [39] Jékely G, Melzer S, Beets I, Kadow ICG, Koene J, Haddad S, Holden-Dye L. The long and the short of it - a perspective on peptidergic regulation of circuits and behaviour. *J Exp Biol* 2018;221:jeb166710.

FIGURE LEGENDS

Figure 1. Distribution of peptide-secreting cells in *Trichoplax adhaerens*.

(A) Cells expressing SIFGamide, SITFamide, TrIns3, RWamide, FFNPamide and YYamide are spatially organized. Maximal intensity projection images illustrate populations of labelled cells (green) for the indicated peptides upon whole-mount immunostaining of *T. adhaerens* individuals. Images show the cumulative positions of labelled cells from above (left panel) and from the side (in a 10 μm slice; middle panel). Representative cells of each population are shown at high magnification in their long axis (horizontal for SIFGamide, SITFamide and RWamide cells, vertical for TrIns3, FFNPamide and YYamide; right panel). The size and distribution of labelled granules widely vary across cell populations. Hoechst-stained nuclei (blue) and auto-fluorescent particles (red) serve as landmarks to locate the upper and lower epithelial layers. (B) Populations of peptidergic cells do not overlap. A maximal intensity projection confocal image illustrates the partitioned distribution of SIFGamide (green), SITFamide (blue) and FFNPamide (red)-immunoreactive cells in *T. adhaerens*. Of note, DAPI staining was recorded in a fourth channel (not shown), and the unspecific labelling common to all four channels, which corresponds to numerous round-shaped auto-fluorescent "concrement vacuoles", was subtracted from the image for clarity. (C) Schematic representation of the respective positions of peptidergic-immunoreactive cell populations in *T. adhaerens*, on top and side views, similar to the planes in A. Of note, SITFamide sera also faintly labelled the mitochondrial clusters of fiber cells (not shown).

*, upper edge of the animal; le, lower epithelium; ue, upper epithelium. Scale bars: in A, 10 μm for the left and middle panels, 4 μm for the right panel; in B, 10 μm . See also Figures S1 and S6 and Table S2.

Figure 2. PWN and SIFGamide elicit partial detachment and folding of *Trichoplax adhaerens*.

Representative images (A, E), trajectory (B, F) and surface area over time (C, G) of *T. adhaerens* individuals upon a single batch application of 20 μM PWN (A-D) or SIFGamide (E-H). (D, H) Average surface area variations (Mean+StDev) upon 20 μM PWN (n=22 animals in 5 trials) or SIFGamide (n=23 animals in 6 trials). Travelling paths (in grey/black: before/after application) do not show major alteration in trajectories, illustrating that *T. adhaerens* remain attached at the bottom of the dish. Scale bars: 250 μm in A, 200 μm in B and F, 170 μm in E. See also Figure S4 and Tables S1 and S2.

Figure 3. LF and LFNE induce rotation and extreme flattening of *Trichoplax adhaerens*.

Representative images (A, E), trajectory (B, F) and surface area over time (C, G) of *T. adhaerens* individuals upon a single batch application of 20 μM LF (A-D) or LFNE (E-H). (D, H) Average surface area variations (Mean + StDev) upon 20 μM LF (n=12 animals in 3 trials) or LFNE (n=22 animals in 5 trials). Travelling paths (in grey/black: before/after application) show drastic changes in trajectories upon peptide application. Not only are individuals rotating around a fixed axis in an unusually "frozen" shape (see arrows in E), but are also moving in small circular paths within

the dish. They periodically underwent massive flattening. Scale bars: 250 μm in A and E, 200 μm in B and F. See also Figure S4 and Tables S1 and S2.

Figure 4. FFNPamide, ELPE, MFPP and WPPF provoke flattening and different forms of "internal" movement, e.g. churning, in *Trichoplax adhaerens*.

Responses of *T. adhaerens* to a single application of 20 μM FFNPamide (A-D), ELPE (E-H), MFPP (I-L) or WPPF (M-P). Representative images (A, E, I, M), area (B, F, J, N) and speed (D, H, L, P) over time of an example individual. Average numbers of flattening events (C, G, K, O) before (0-15' (ctrl)) and after peptide application (15-30', 30-45')(Mean+StDev). For FFNPamide (C), n=20 animals in 3 trials; for ELPE (G), n=42 animals in 5 trials; for MFPP (K), n=39 animals in 5 trials; for WPPF (O), n=46 animals in 4 trials. While all 4 peptides invariably yield more frequent flattening, each of them induces specific alterations in shape and movements that can be observed in the Suppl. video material. Scale bars: 250 μm in A, E and I, 170 μm in M. Statistical tests applied: Wilcoxon for FFNPamide, ELPE, WPPF; Mann-Whitney for MFPP; ns, non-significant; *, p<0.05; **, p<0.01; ***, p<0.001; ****, p<0.0001. See also Figures S2-5 and Tables S1 and S2.

STAR Methods

CONTACT FOR REAGENT AND RESOURCE SHARING

Further information and requests for resources and reagents should be directed to and will be fulfilled by Dirk Fasshauer (dirk.fasshauer@unil.ch).

EXPERIMENTAL MODEL AND SUBJECT DETAILS

Animal Maintenance

Trichoplax adhaerens (Grell strain, haplotype H1) were maintained in large glass Petri dishes (15-cm diameter) containing artificial seawater (filtered ASW, salinity of 1025 ppm (38 g/l) salinity; Coral Pro Salt, Red Sea), at 26°C and under a 12:12 hr dark-light cycle. They were fed once a week with 8-10 ml of a 1:1 mixture of *Nannochloropsis* (Florida Aqua Farms) and *Pyrenomonas helgolandii* (SAG, Göttingen, Germany) cultured separately in ASW complemented with 0.03 % of Micro Algae Grow (Florida Aqua Farms). About 80 % of the medium was replaced every other week. When reaching a population density of over 100-200 individuals per dish, 10 to 20 animals were randomly taken up with a pipette to set up a new dish. The animals reproduce asexually and their sex was not determined.

METHOD DETAILS

Antibody production

Polyclonal antibodies were generated in rabbits (2 rabbits per peptide, Speedy program, Eurogentec) against peptide candidates [11,12] that were predicted to be amidated, namely "FFNPamide" (CQFFNP-amide), "RWamide" (CRDQPPRW-amide), "SIFGamide" (CQANLKSIFG-amide), "SITFamide" (CNSESTQQGIPSITF-amide), "YYamide" (CGYDDYYY-amide), and Insulin-3 "TrIns3" (CPIH-amide). For immunization, peptides were coupled to ovalbumin as carrier protein; the cysteine

residue added at the N-terminal of the peptides allows for subsequent immobilization on a Sulfolink resin (ThermoFisher). Sera were affinity-purified as described [14], each resulting in two fractions after elution at pH2.9 and pH2.3. Initial immunostainings were carried out with crude and purified antibodies. The two sera raised against each peptide gave similar staining patterns; In all cases, stainings were invariably abolished upon pre-incubation of the primary antibody with the peptide it was raised against.

Immunolabelling

T. adhaerens were left to adhere at the bottom of 35-mm plastic Petri dish filled with ASW, swiftly replaced by 4 % paraformaldehyde (PFA) with Dextran in ASW for fixation (1-2 hrs, RT). After brief washes in ASW followed by 0.1 M phosphate buffer pH7.4 (PB) and a 1 hr-blocking step in 3 % normal goat serum (NGS) + 0.2 % Triton X-100 in PB, they were incubated for 2 hrs in primary antibody (anti-peptide: 1 µg/ml; anti-FMRFamide (1:300; Enzo Life Sciences #BML-FA1155 or Phoenix Pharmaceuticals #H-047-29) in blocking solution. After thorough washes in PB, a 1-hr incubation in the corresponding secondary antibody coupled to a fluorophore (1:600, GAR-Alexa Fluor, Molecular Probes) and further washes in PB, they were incubated for 2 minutes in Hoechst (1:10,000; Molecular Probes), rinsed and mounted with Prolong-Gold (LifeTech) on glass slides. For co-labelling with antibodies raised in the same species, *T. adhaerens* were instead incubated 45 minutes in a mix of antibodies coupled to Alexa fluorophores using the Zenon labelling kit (LifeTechnologies) following the manufacturer's instructions, washed in PB, post-fixed 15 minutes in 4 % PFA, washed again and incubated in Hoechst before being mounted on a slide. For blocking experiments, we pre-incubated the antibodies in three times excess of the respective peptides for 2 h before immunostainings.

Imaging

Specimens were imaged on an inverted confocal microscope set-up (Zeiss LSM 780) using a 63x-oil immersion objective (NA1.4). Image stacks were acquired over the entire thickness of the animal with optical slices of 1.3 µm with an overlap of 0.75 µm, with each fluorophore imaged separately.

Behavioural testing

Most peptides were dissolved in water, except for YYamide and LF, which were dissolved in 5 mM NH₄HCO₃. 10-15 *T. adhaerens* were pipetted into a 35-mm plastic Petri dish filled with 3 ml ASW and allowed to settle for 15-30 minutes at 26°C. The dish was then transferred to the stage of a stereomicroscope (Nikon SM225 coupled to a Nikon DSR12 camera) with a zoom of 0.63x or 3x, and imaged for 50 minutes. After 15 minutes, each peptide (200 nM - 50 µM from a 10 mM stock solution) was applied once and swiftly mixed in the bath by gentle pipetting. Peptides tested were the following: "ELPE" (GKSFELPE), "FFNPamide" (DDQFFNP-amide), Insulin-3 "TrIns3" (CPIH-amide), "LF" (DDSQDGYALF), "LFNE" (QEPGISLFNE), "MFPF" (EDDLPGMFPF), "PWN" (EQGALLDIPWN), "RWamide1" (DQPPRW-amide), "RWamide2" (DQPTRW-amide), "RWamide3" (DQPSRW-amide), RWamides bearing a N-term pyroGlutamine modification "pGluRWamide1-3", "SIFGamide" (EDQANLKSIFG-amide), "SITFamide" (NSESTQQGIPSITF-amide), "WPPF" (EDQQNKPYNGWPPF), and "YYamide" (DYDDYYY-amide) (see Table S1 and S2 for details). Control experiments were carried out by application of the vehicles only. Endomorphin-2 (Genscript, RP10926) was tested at concentrations of 1, 15 and

50 μ M. Images were taken every 4 seconds under moderate and constant illumination, and at a room temperature of approximately 20°C. Upon recording, the dishes were placed back in the incubator with food to check animal viability 24 hrs after treatment.

QUANTIFICATION AND STATISTICAL ANALYSIS

Image Analysis and Statistical Methods

Black and white image series (Tif) were analysed with Fiji. Only individuals that were visible during the entire time of the recording were tracked. Since animals in close contact may coordinate their behaviours [17,24], only animals which were not in contact with one another were monitored to avoid oversampling. In rare cases when individuals were in contact with each other, only one was monitored. Images on which the application pipettes appeared were not taken into account for analysis. The maximum trajectory area was set as ROI for each individual and a time stamp applied (see .avi videos as Supplemental information). A threshold (Yen, Fiji) was set to optimally define the contour of each individual, allowing for the binarization of the image and measurement of the animal's size (area) using the Plugin 'Analyse Particles' in Fiji. Trajectory, distance covered and speed were assessed from the centroid, using the 'Mtrack2' Plugin in Fiji. To standardize area variations over several animals, the average area was defined for each individual over the first 15 minutes of recording and used as a baseline to normalize the values over the recording. Standard deviations /Standard Errors of the Mean were calculated for each time point for all individuals using Excel or Prism. Results are presented as Mean \pm StDev in Figure 4, Mean \pm SEM in Figures S3 and S5. When the values followed a normal distribution, a paired t-test was used (Figures S3 and S5). Otherwise, a paired Wilcoxon test was applied (Figure 4).

Video files

Movie S1: Time-stamped videos showing examples of *T. adhaerens*' behaviour upon application of 20 μ M PWN.

Movie S2: Time-stamped videos showing examples of *T. adhaerens*' behaviour upon application of 20 μ M SIFGamide.

Movie S3: Time-stamped videos showing examples of *T. adhaerens*' behaviour upon application of 20 μ M LF.

Movie S4: Time-stamped videos showing examples of *T. adhaerens*' behaviour upon application of 20 μ M LFNE.

Movie S5: Time-stamped videos showing examples of *T. adhaerens*' behaviour upon application of 20 μ M FFNPamide.

Movie S6: Time-stamped videos showing examples of *T. adhaerens*' behaviour upon application of 20 μM ELPE.

Movie S7: Time-stamped videos showing examples of *T. adhaerens*' behaviour upon application of 20 μM MFPPF.

Movie S8: Time-stamped videos showing examples of *T. adhaerens*' behaviour upon application of 20 μM WPPF.

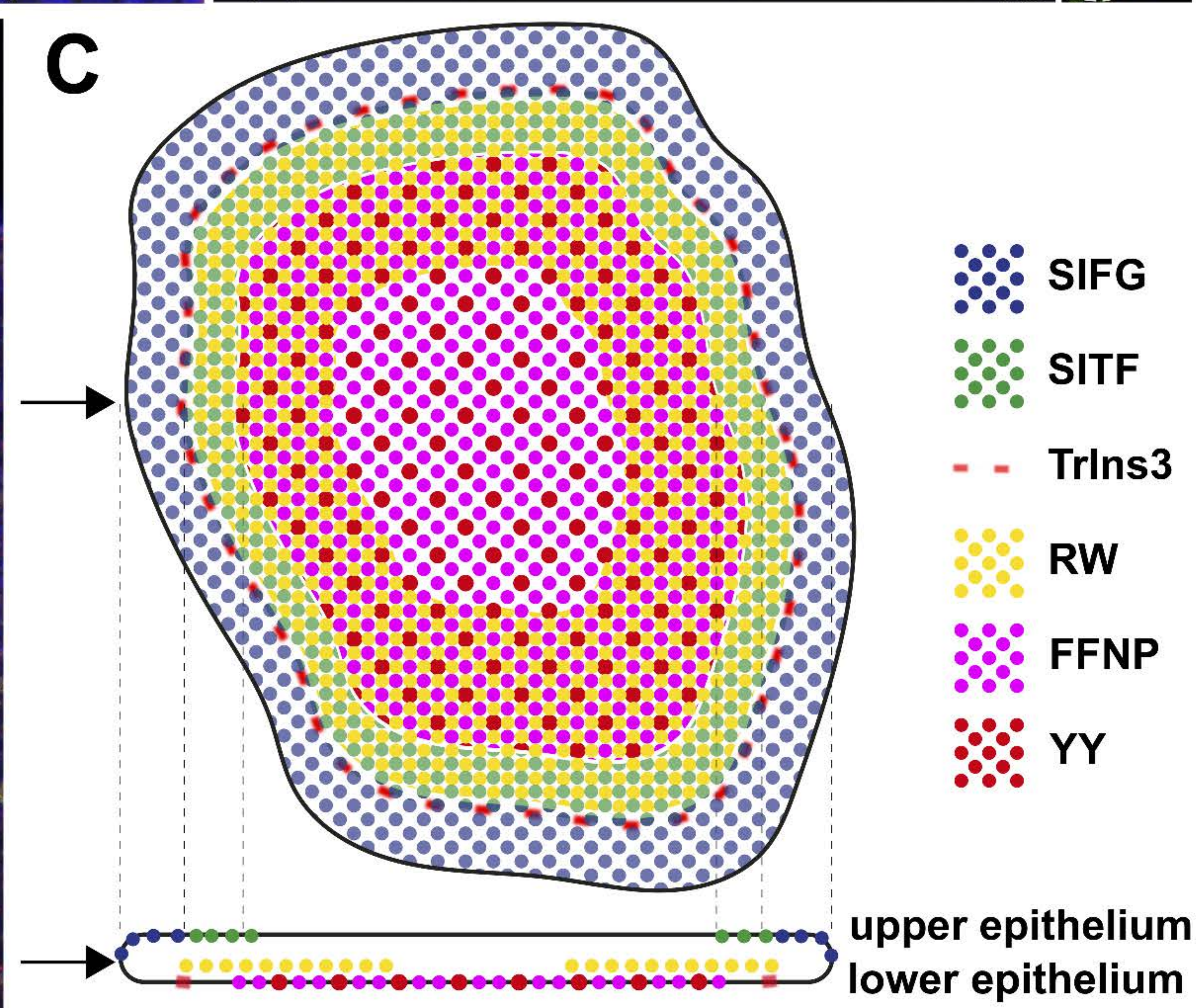
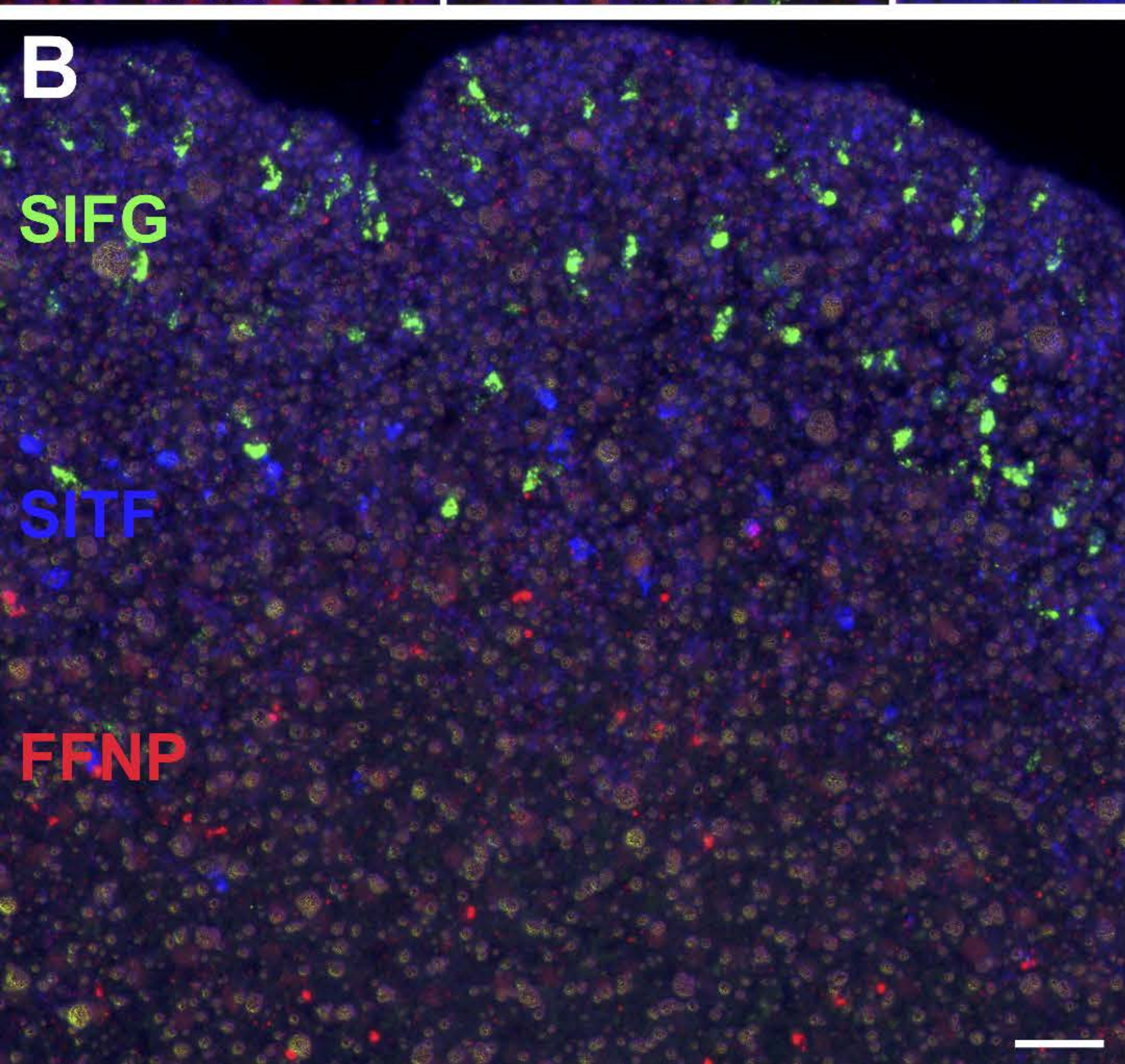
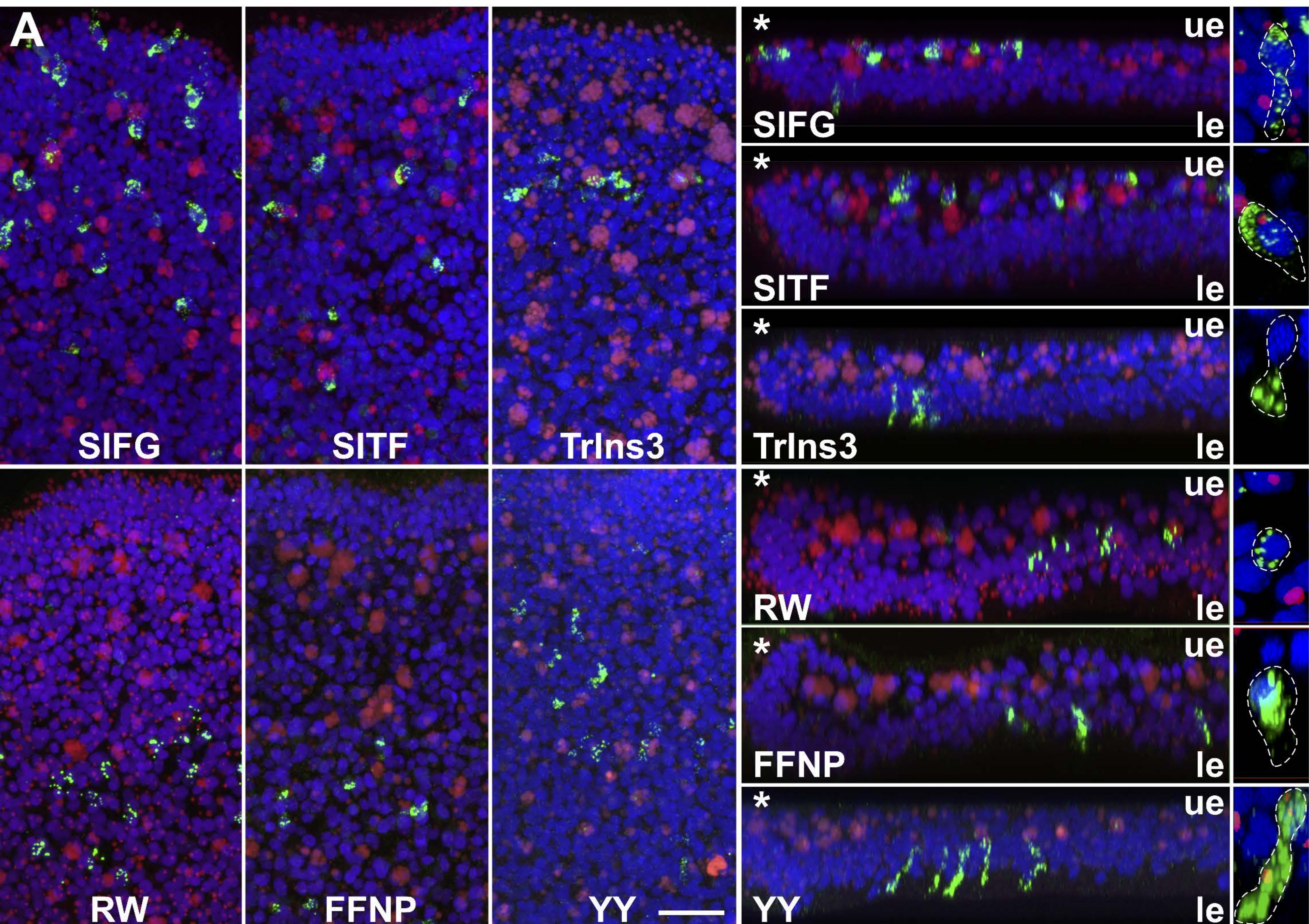
Movie S9: Time-stamped videos showing examples of *T. adhaerens*' behaviour upon application of 20 μM SITFamide.

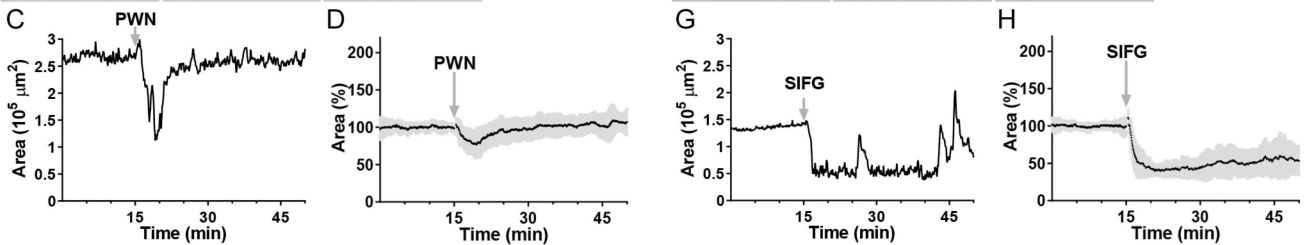
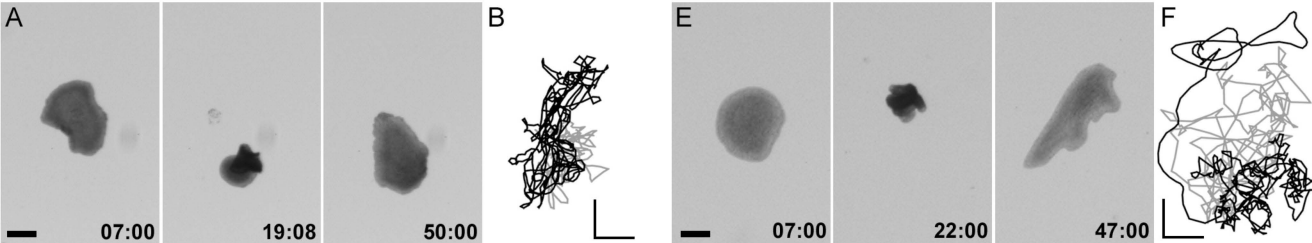
Movie S10: Time-stamped videos showing examples of *T. adhaerens*' behaviour upon application of 20 μM YYamide.

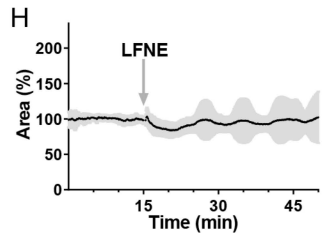
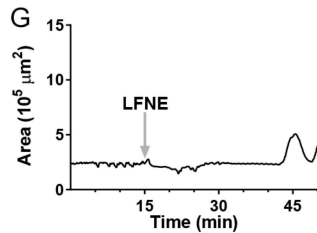
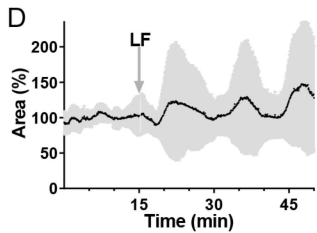
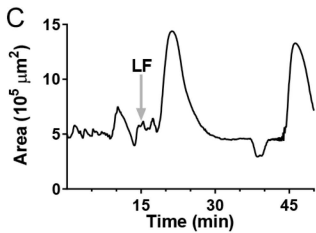
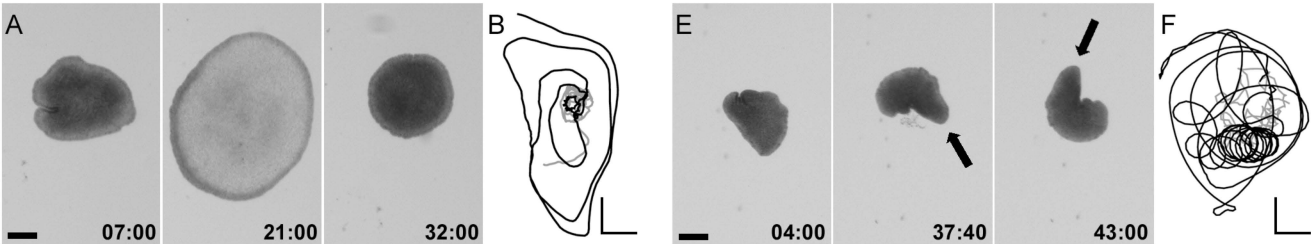
Movie S11: Time-stamped videos showing examples of *T. adhaerens*' behaviour upon application of 20 μM pRWamide2.

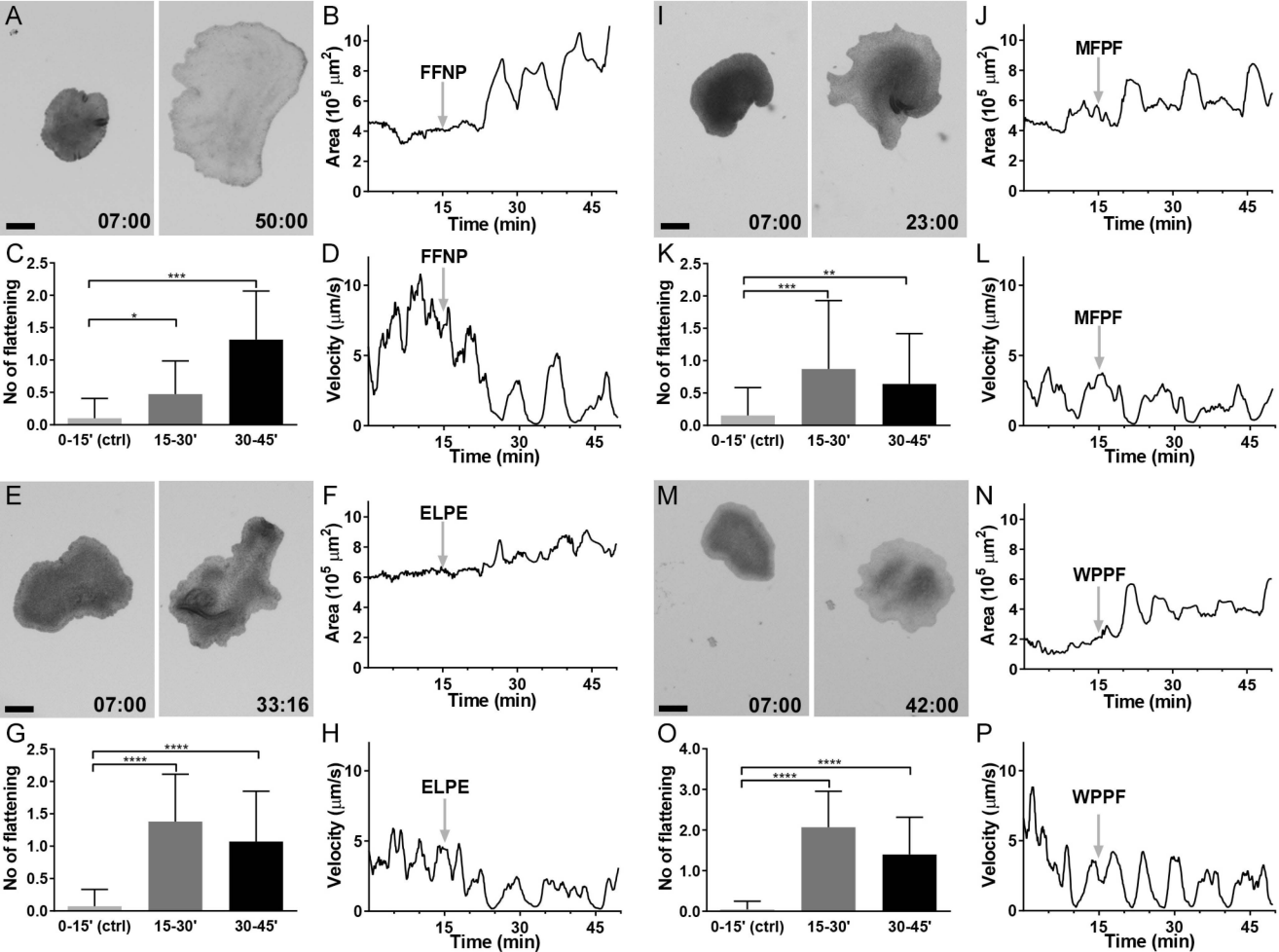
Movie S12: Time-stamped videos showing examples of *T. adhaerens*' behaviour upon application of H_2O .

Movie S13: Time-stamped videos showing examples of *T. adhaerens*' behaviour upon application of NH_4HCO_3 .









SUPPLEMENTAL FIGURES

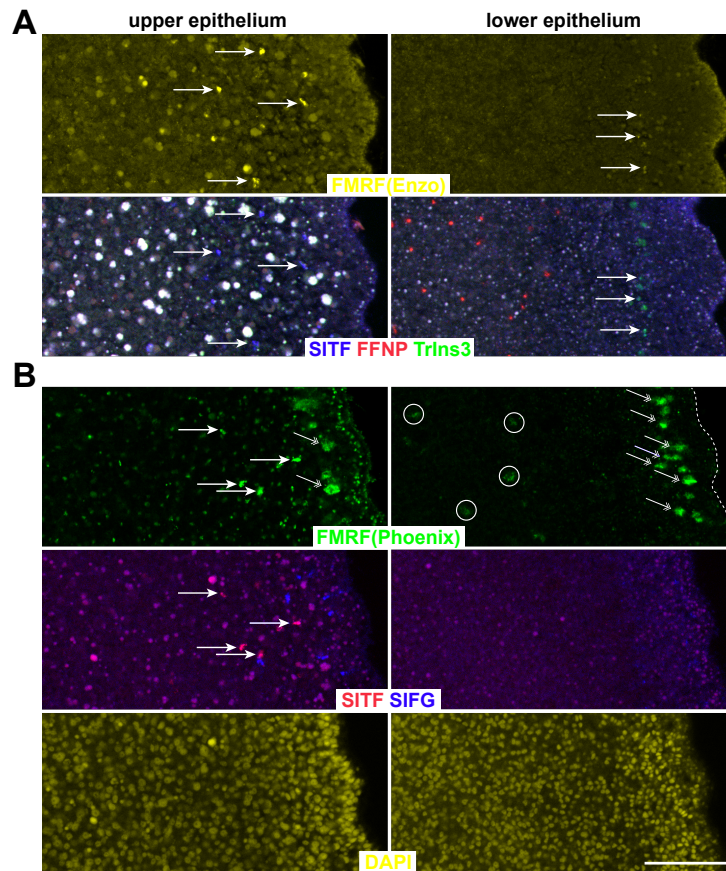


Figure S1. Different antibodies against FMRFamide co-label SITFamide-immunoreactive cells. Related to Figure 1.

Anti-FMRFamide antibodies from Enzo (#BML-FA1155; yellow in A) and from Phoenix labs (#H-047-29, lot 01479-1; green in B) were used in combination with other peptide antibodies. Labelling is illustrated in a single optical slice of the upper epithelium (left column) and the lower epithelium (right column) of the same image stack.

(A) Quadruple staining for FMRFamide from Enzo (FMRF(Enzo), yellow, upper panels), SITFamide, FFNPamide and TrIns3 (blue, red and green, lower panels) shows that this FMRFamide antibody strongly co-labels SITFamide-immunoreactive cells and to a lesser extent, TrIns3-stained cells (arrows). Populations of immunoreactive cells for SITFamide, FFNPamide and TrIns3 do not overlap. Of note, the numerous round-shaped white particles observed predominantly in the upper epithelium are autofluorescent "concrement vacuoles".

(B) Quadruple staining for FMRFamide from Phoenix (FMRF(Phoenix), green, upper panels), SITFamide and SIFGamide (red and blue, middle panels) and Hoechst (yellow, lower panels) shows that this FMRFamide antibody also strongly co-labels SITFamide-immunoreactive cells (arrows) but not SIFGamide-stained cells. This antibody also labels a row of large cells located close to the edge of the organism (double-arrowheads) and some scarce cells of the lower epithelium (circles) likely corresponding to another population of unidentified gland cells [8], as well as small unidentified elements in the upper epithelium. Populations of immunoreactive cells for SITFamide and SIFG do not overlap. Note again the presence of autofluorescent particles, visible in all channels, and the difference of Hoechst-stained nuclei size and number across both epithelia.

Scale bar: 30 μm .

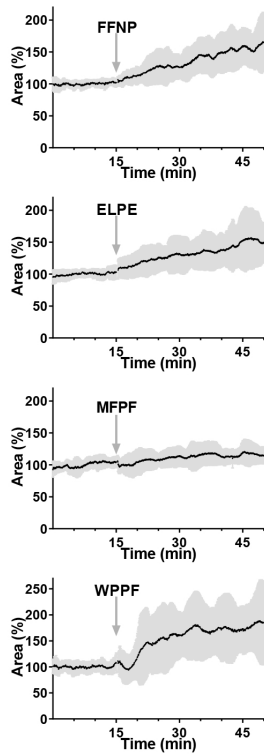


Figure S2. Average area over time upon application of FFNPamide (n=17), ELPE (n=24), MFPP (n=17), WPPF (n=18). Related to Figure 4. A single peptide application (arrow) induced a sustained increase of the standard deviation, reflecting an effect of the peptide.

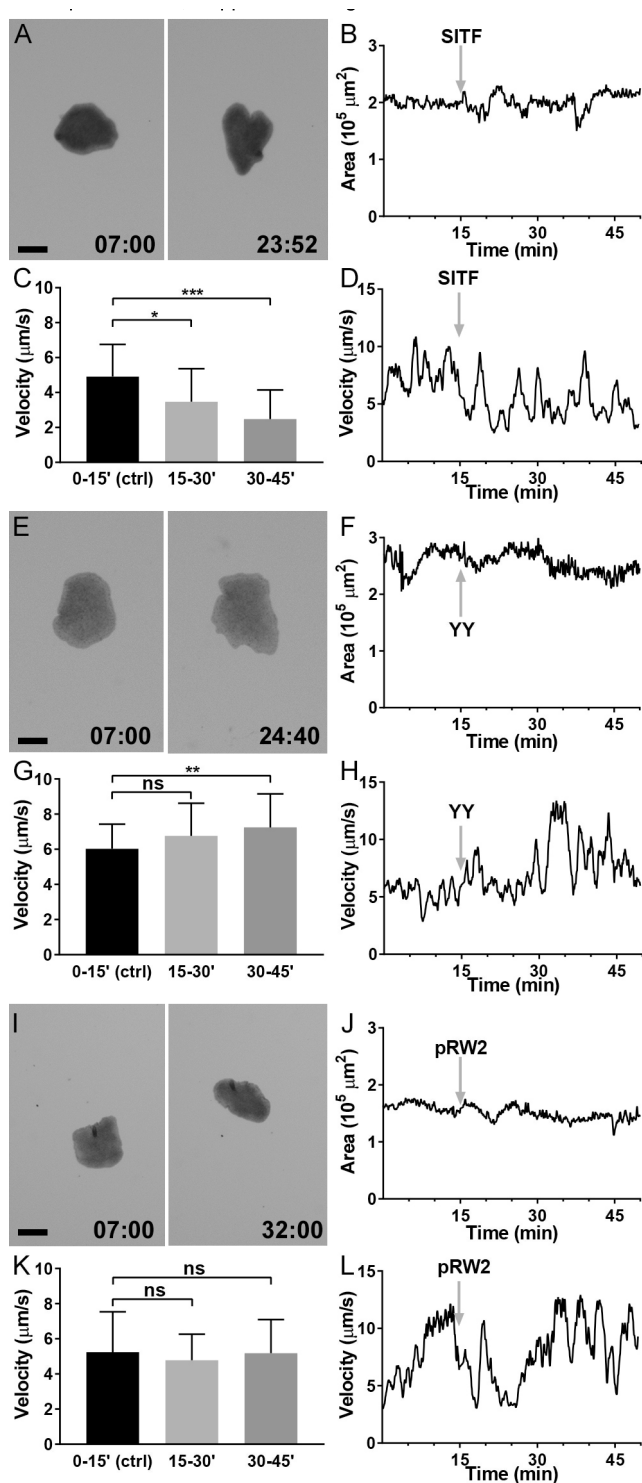


Figure S3. Subtle effects of SITFamide, YYamide or pRWamide2 application to *Trichoplax adhaerens*. Related to Figure 4.

Responses of *T. adhaerens* to a single application of 20 μM SITFamide (A-D), YYamide (E-H) or pRWamide2 (I-L). Representative images (A, E, I), area (B, F, J) and speed (D, H, L) over time of an example individual. (C, G, K) Average velocities (C, SITFamide, $n=15$; G, YYamide, $n=15$; pRWamide2, $n=15$) before (0-15' (ctrl)) and after peptide application (15-30', 30-45') (Mean+StDev). Scale bars: 250 μm in A, E and I. Statistical tests applied: Wilcoxon for SITFamide, Mann-Whitney for YYamide and pRWamide2; ns, not significant; *, $p<0.05$; **, $p<0.01$; ***, $p<0.001$; ****, $p<0.0001$.

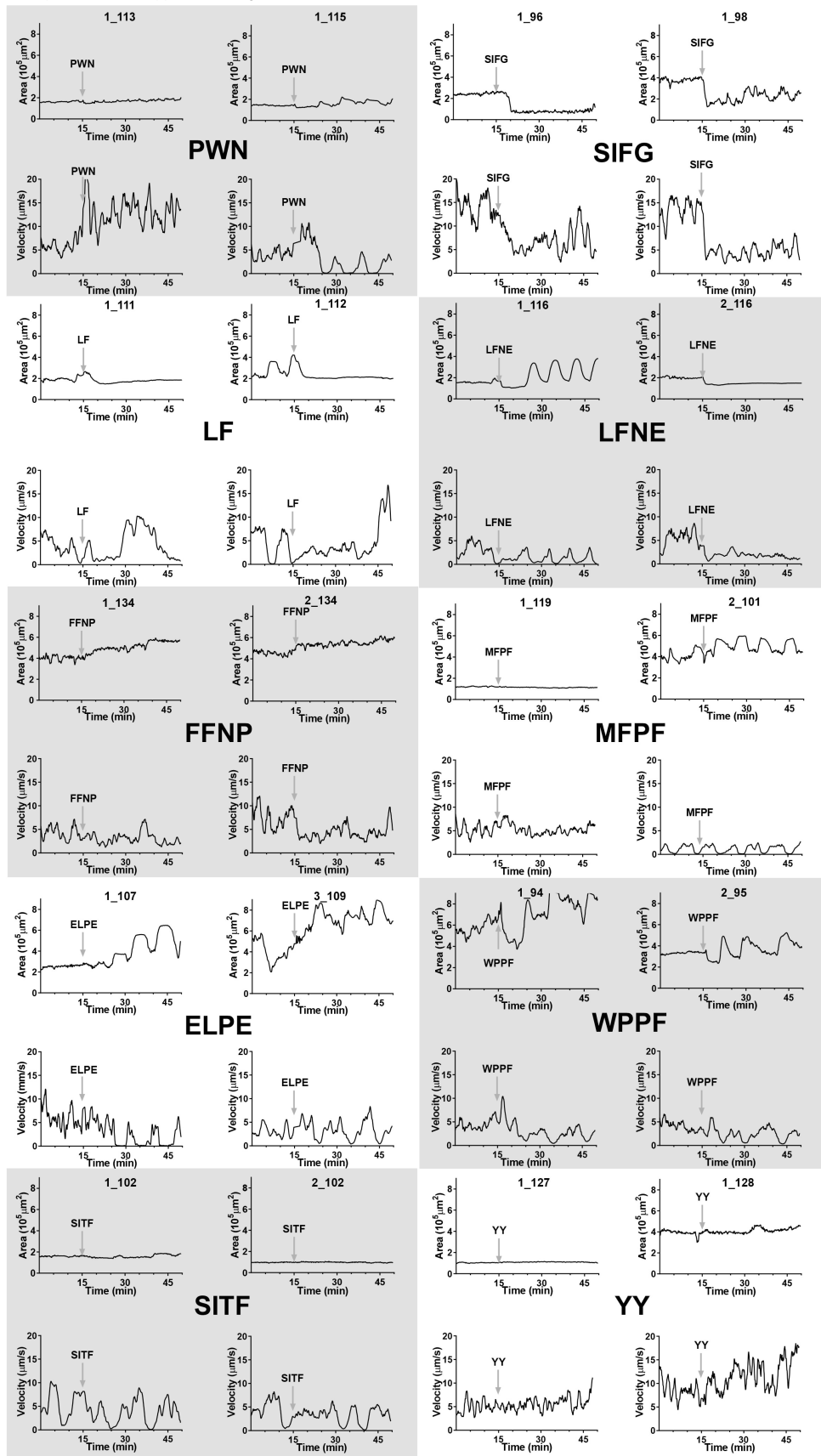


Figure S4. Example traces of behaviours (area and speed) of *T. adhaerens* individuals upon application of the indicated peptides. Related to Figures 2-4.

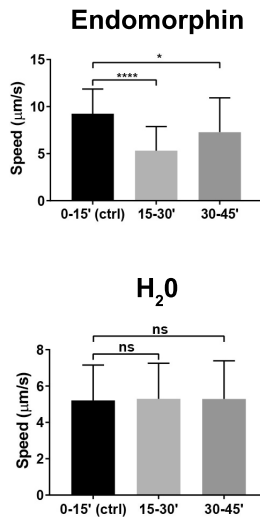


Figure S5. Average speed upon application of endomorphin-2 (n=14) or H₂O (n=16). Average speed before (0-15' (ctrl)) and after H₂O or endomorphin application (15-30', 30-45') (Mean+SEM). Statistical test applied: Paired t-test; ns, not significant; *, p<0.05; **, p<0.01; ***, p<0.001; ****, p<0.0001. Related to Figure 4.

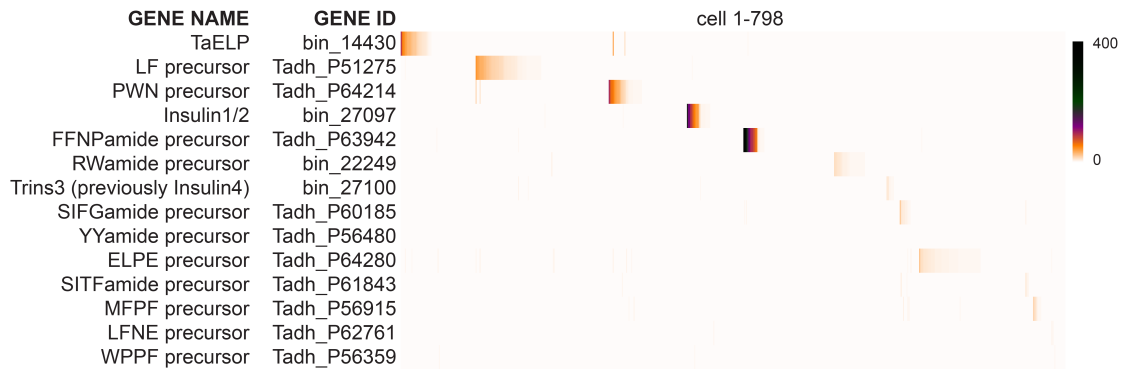


Figure S6. Expression of *Trichoplax* neuropeptide-precursor-like sequences in single cells. scRNAseq data from Seb e-Pedr s et al. [34] were sorted by propeptide normalized expression level. 798 cells out of 3,209 single cells expressed at least one of the listed peptides. Data were retrieved from GEO Accession: GSE111068. Related to Figure 1.

Neuropeptide acronym	Neuropeptide sequence	Concentration tested *					
		200 nM	1 μ M	5 μ M	10 μ M	20 μ M	50 μ M
ELPE	GKSFELPE	- (1; 2/8)	- (2; 0/23)	+ (1; 12/0)	+ (1; 8/1)	+ (10; 59/12)	
FFNPamide	DDQFFNPamide			- (1; 4/10)	+ (1; 6/5)	+ (5; 29/9)	
LF	DDSQDGYALF	+ (1; 7/2)	+ (1; 5/2)	+ (1; 10/1)	+ (1; 10/0)	+ (5; 49/0)	
LFNE	QEPGISLFNE	+ (1; 8/3)	+ (1; 19/0)	+ (1; 13/0)	+ (1; 9/0)	+ 8; 71/3)	
MFPF	EDDLPGMFPPF	- (1; 0/3)	+ (2; 9/8)	+ (1; 12/0)	+ (1; 11/0)	+ (8; 43/22)	
PWN	EQGALLDIPWN	- (1; 0/7)	+ (2; 18/1)	+ (1; 11/2)	+ (1; 7/1)	+ (8; 32/26)	
pRW2amide	pyro-QPTRWamide					- (2;0/15)**	
SIFGamide	EDQANLKSIFGamide	+ (1; 8/0)	+ (1; 13/0)	+ (1; 10/0)	+ (1; 9/0)	+ (7; 74/0)	
SITFamide	NSESTQQGIPSITFamide	+ (1; 9/0)	+ (2; 17/0)	+ (1; 13/0)	+ (1; 12/0)	+ (2; 16/2)	
WPPF	EDQQNKPYNGWPPF	- (1; 2/11)	+ (3; 17/3)	+ (1; 8/0)	+ (1; 10/0)	+ (5; 55/2)	
YYamide	DYDDYYYamide			+ (1; 12/0)	+ (1; 11/0)	+ (2; 10/0)	
Endomorphin-2	YPPF		+ (1;4/0)			+ (1;10/4)***	+ (2;17/0)

crinkling

rounding up and rotating

flattening and churning

Table S1. Summary of the peptides tested. Related to Figures 2-4.

The number of independent trials carried out for a given peptide at a given concentration, as well as the number of animals showing or not the described phenotype (see color code) are given. Note that the numbers of individuals reported in the main analyses were often lower as only animals observable during the entire time of the recording and not touching each other were used for quantification.

* +/- (x;y/n) effect or no effect (number of independent trials; number of responsive animals/ non-responsive animals)

** pilot experiments were carried out with RW1amide, RW2amide, RW3amide, pRW1amide, pRW2amide and pRW3amide, which showed no drastic effect.

*** tested at 15 μ M

